Journal of Power Sources 198 (2012) 190–195

Contents lists available at SciVerse ScienceDirect

Journal of Power Sources

journal homepage: www.elsevier.com/locate/jpowsour

A strategy for facile durability improvement of perfluorosulfonic electrolyte for fuel cells: Counter ion-assisted decarboxylation at elevated temperatures

Yuting Cheng, Haolin Tang*, Mu Pan

State Key Laboratory of Advanced Technology for Materials Synthesis and Processing, Wuhan University of Technology, Wuhan 430070, PR China

ARTICLE INFO

Article history:
Received 30 September 2011
Accepted 6 October 2011
Available online 13 October 2011

Keywords:
Perfluorosulfonic acid
Chemical durability
Decarboxylation
Temperature
Counter ion

ABSTRACT

A strategy for improving the chemical stability of perfluorosulfonic acid is proposed by hydrothermal decarboxylation of defect groups with the assistance of counter ions and ethylene glycol at elevated temperatures. An apparent decrease in the carboxyl end groups is observed at decarboxylation temperatures of 180–220 °C. Decarboxylation of perfluorosulfonic acid significantly improves the chemical stability of the perfluorosulfonic electrolyte toward hydroperoxyl radicals, resulting in high concentrations of S_{2p} and F_{1s} after radical corrosion for 12 h. The decarboxylation of the electrolyte at elevated temperature also improves the side chain stability of the perfluorosulfonic acid. The fluoride emission rate decreases with increased decarboxylation temperature, implying a low side chain cleavage of the perfluorosulfonic acid polymer.

1. Introduction

Proton exchange membrane (PEM) degradation continues to present challenge for fuel cells to meet the required lifetime. This is especially the case when the fuel cell is operated in transportation applications with extreme or cyclic changes in load [1,2]. In addition to physical and mechanical degradations, membrane degradation by hydroxyl and hydroperoxyl radicals was found to be responsible for membrane chemical degradation [3–5]. Perfluorosulfonic acid (PFSA) membranes, such as Nafion, are deemed as the state-of-art PEM materials because of its excellent chemical stability and relatively high proton conductivity when fully hydrated [6]. However, small amounts of carboxyl end groups remain in the perfluorosulfonic acid, which act as defect groups subject to hydroperoxyl radicals [7]. Under this condition, defect carboxyl end groups are oxidized to carbon dioxide, reforming the linked CF_2 units to another terminal carboxyl group and result in unzipped degradation [8,9]. Thus, chemical destruction and performance degradation of the Nafion membrane are frequently observed in fuels cells that have been operated for long or accelerated periods [10,11].

In the past several years, much effort has been geared toward the development of alternative, chemically stable PEMs. Cross-linked polyelectrolyte [12], grafted copolymer electrolyte [13], and multilayer electrolytes with aromatic polymers [14] fall into this category. Although each material has its own advantages, most are restricted by the imbalance of physical stability and proton conductivity of the electrolyte membrane due to the inherently low conductivity of the hydrocarbon electrolyte. Another approach is to introduce an abnormal valence catalyst such as cerium oxide [15,16], manganese oxide [17], heteropoly acids [18], or zirconia [19] into the proton exchange membrane to decompose the hydroperoxyl radicals during operation. However, the oxides are potentially soluble with the production of water in the fuel cell, and the reducing energy conversion efficiency is also a concern because of the oxidation of intermediates.

It was reported that the carboxyl end groups could be removed from organic hydrocarbons with the presence of counter ions as the catalyst, and the reaction kinetics could be much improved at elevated temperatures [20]. For small perfluorocarbon molecules, the carboxyl end groups also can be converted to a stable hydrogenated state with the assistance of potassium salts [21]. For perfluorosulfonic acid, our previous research demonstrated that the electrolyte membrane prepared from NaOH neutralized ionomers at elevated temperatures have better chemical stability compared with commercial membranes [22]. Here, we report a facile durability improvement strategy for perfluorosulfonic acid by hydrothermal decarboxylation of defect groups with the assistance of counter ions and ethylene glycol at elevated temperatures. The effects of the reaction temperature on decarboxylation efficiency and the chemical stability of the polymer were also systematically investigated and discussed.

* Corresponding author. Tel.: +86 27 8788 4448; fax: +86 27 8787 9468.
E-mail address: tanghaolin2005@yahoo.com.cn (T. Haolin).

0378-7753/$ – see front matter © 2011 Elsevier B.V. All rights reserved.
doi:10.1016/j.jpowsour.2011.10.021

2. Experimental procedures

2.1. Hydrothermal decarboxylation of the perfluorosulfonic acid ionomers

Prior to the reaction, Nafion ionomers (Nafion DE 520, EW value = 1000, 5 wt.% Nafion, 45 ± 5 wt.% water and 48 ± 6 wt.% 1-propanol, DuPont) were converted to Na^+ form by slowly adding NaOH solution (0.1 mol L^{-1}) until the pH reached 7.0–7.5. Then, the Nafion ionomers were transferred to an ethylene glycol (EG) solution by distilling a mixing solution containing 500 mL Nafion solution and 500 mL ethylene glycol until the solution temperature reached 190 °C to remove any organics with a low boiling point. The solution was then transferred into Teflon-lined stainless autoclaves and maintained at 150–220 °C for 24 h for decarboxylation.

The recasting proton exchange membrane was made by transferring the resulting solution into a Petri dish, dried in a vacuum oven at 90 °C, followed by heat treatment at 130 °C and 200 °C. The membranes were finally converted to H-form by using a standard procedure of 5 wt.% H_2O_2 solution, then distilled water at 80 °C, followed by 0.5 M H_2SO_4 solution at 80 °C, and finally distilled water at 80 °C at; all at 80 °C each step was performed for 30 min each.

2.2. Characterization and chemical stability of the electrolyte membrane

IR spectrum was recorded on a spectrometer (FTIR-4200, Nexus) with a resolution of 4 cm^{-1} in the range of 400–4000 cm^{-1}. For the membrane characterization, the samples were sandwiched between two KBr plates and placed in the cell for measurement. All the samples had a standard size of 3.5 cm × 1.5 cm to cover the whole window, preventing any interference. Prior to the FTIR test, the membrane samples were dried at 90 °C for 8 h to minimize the water content in the samples.

Raman spectra were obtained by excitation with radiation of wavelength 532.0 nm from an Ar–YAG laser operating at approximately 20 mW. The spectra were recorded at room temperature using a LABRAM 1B confocal Raman spectrometer (Renishaw, inVia, UK) equipped with a charge-coupled device detector cooled with a Peltier cooler. The spectrometer was coupled to the experimental cell described above with an Olympus microscope at 100× magnification. The in-depth resolution of the objective, as estimated under the experimental conditions applied in this study, is 7 ± 1 μm. The scan step used in this study was 1.25 μm. The volume of the sample probed by the focalized laser beam at each step of the Raman cartography was 14 μm^3.

The EW value of the membrane was measured by titrating the NaCl solution (after ion exchange with the membrane) with 0.1 M NaOH solution. Titration was repeated at least three times to confirm the reproducibility of the results. Proton conductivity of the recasting membranes was measured using an impedance analyzer (Autolab PG30/FRA, Eco Chemie, the Netherlands) at 25 °C, 100% RH. The membrane (6 cm × 1 cm) was sandwiched between two Pt sheets. One Pt sheet was used as the working electrode and the other as the reference and counter electrodes. Electrochemical impedance spectroscopy (EIS) was performed in the frequency range of 10–100 kHz under a signal amplitude of 10 mV.

Surface morphology of the composite membranes was examined by scanning electron microscopy (SEM; JEOL JSM-5610LV). The samples were Au-sputtered under vacuum before SEM examination.

XPS spectra were collected using a Physical Electronics (PHI) Model 1600 XPS system equipped with a monochromator and an Al Kα source ($h\nu$ = 1486.8 eV) operated at 350 W beam power. Ejected photoelectrons were detected by a hemispherical analyzer that provided both high sensitivity and resolution. The operating pressure in the sampling chamber was below 5 × 10^{-9} Torr. A neutralizer beam was used during XPS measurements to compensate for peak shifting that occurs due to charging of samples during X-ray exposure. All high-resolution spectra were collected using pass energy of 46.95 eV. The step size and time per step were 0.025 eV and 100 ms, respectively. The samples were scanned at different locations, and the peak intensity and composition at different locations were compared to assure uniformity of film composition over the sample surface.

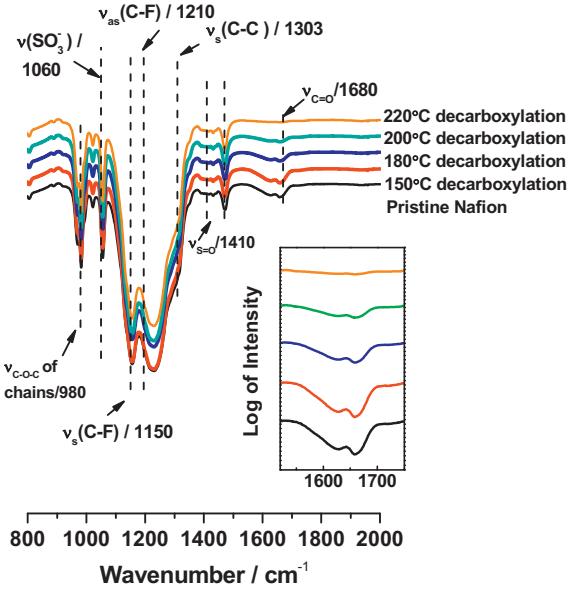

Fig. 1. FTIR spectra of the perfluorosulfonic acid decarboxylated at various temperatures for 24 h. The inset is the magnified adsorption of the carboxyl group located at 1650 cm^{-1}.

The radical corrosion of the electrolyte membranes was conducted by immersing the membranes in 30 wt.% H_2O_2 solution containing 20 ppm $FeCl_2$ (Fenton's reagent solution) at 80–90 °C in a water bath. The solution was collected and replaced by fresh solution every 30 min. The F^- ion emersion rate (amount of F^- cumulated in the Fenton's reagent solution) was analyzed with an ion chromatograph (DIONEX, DX-320). The collected solution was concentrated to 30 mL prior to the test. The condenser, trap and tubing materials in contact with water or gases were made of polypropylene.

3. Results and discussion

3.1. Decarboxylation of the perfluorosulfonic acid electrolyte

Fig. 1 displays the FTIR spectroscopy of the perfluorosulfonic acid ionomers decarboxylated at various temperatures for 24 h. Bands at 1410 and 800 cm^{-1} were assigned as the S=O and S–OH stretching bands of the $-SO_3H$ group. The symmetric $-SO_3$ stretching band is visible at about 1060 cm^{-1}. Vibrational bands of the $-SO_3H$ and $-SO_3$ groups clearly demonstrated that the sulfonic groups were properly protected due to the strong electrostatic interactions of the Na^+ counter ions. The intensity ratio between the vibrational bands of $-SO_3H$ and the absorption bands of $-CF_2$ groups (1150 and 1210 cm^{-1}) show slight improvement, suggesting that the ionomers were reformed to a structure with low constraint on the side chain. Thus, the $-SO_3$ group linked to the side chains was activated and played a positive role in the proton transportation.

Weak bands located at 1650 cm^{-1} and magnified in the insert of Fig. 1 demonstrated that the defect end groups of carboxyl group (–COOH) existed in the pristine perfluorosulfonic acid ionomers

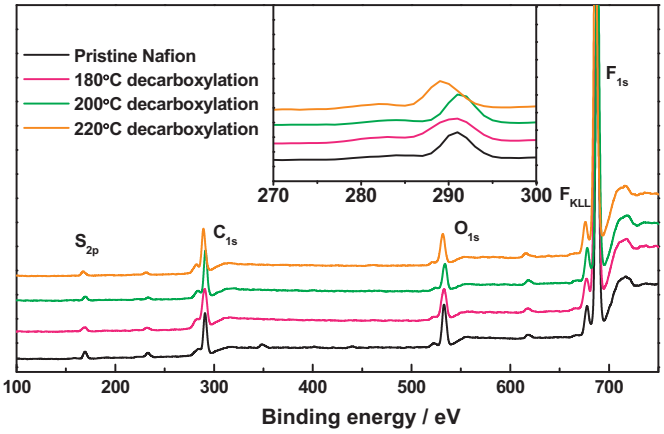

Fig. 2. XPS spectra of the perfluorosulfonic acid decarboxylated at various temperatures for 24 h. The inset is the C_{1s} bands in the 270–300 eV region.

[23]. The adsorption intensity decreased after reacting at elevated temperatures, indicating the efficiency of decarboxylation with the Na+ counter ion as a catalyst:

$$HOOC - CF_2 - R_f + NaOH \xrightarrow{k1} NaOOC - CF_2 - R_f + H_2O \quad (1)$$

$$NaOOC - CF_2 - R_f + H_2O \xrightarrow{k2} H - CF_2 - R_f + H_2O + NaHCO_3 \quad (2)$$

$$2NaHCO_3 \xrightarrow{k3} Na_2CO_3 + CO_2 + H_2O \quad (3)$$

$$2HOOC - CF_2 - R_f + Na_2CO_3 \xrightarrow{k4} 2NaOOC - CF_2 - R_f + CO_2 + H_2O \quad (4)$$

As the decarboxylation temperature increased, the carboxyl group adsorption bands in the FTIR spectrum rapidly decreased, especially at temperatures above 200 °C, indicating that the overall reaction rate had improved at the elevated temperature. For the neutralization reactions (Eqs. (1) and (4)) as well as the decomposition reaction (Eq. (3)), the reaction rates were very rapid with high kinetic constants. Thus, decarboxylation is restricted according to Eq. (2) by a low kinetic constant, κ_2. It is reported that the hydrogen substitution in organic acids is an endothermic reaction [24–26]. Thus, the increase in reaction temperature and reaction time are favorable for improving the carboxyl conversion rate.

The conversion of carboxyl group to the stable carbon–hydrogen bonds was also confirmed in the XPS spectrum (Fig. 2). Fluorine rich carbon configurations, such as $(CF_2)_n$, yield signals at high binding energies. With decreasing fluorine concentration, the carbon signal approached low binding energies [27]. The binding energies of C_{1s} signals were in the energy range of 292.2 eV (for carbon in the CF_2 configuration) to 284.2 eV (for carbon in the C–C or C–H configuration). With the decarboxylation of perfluorosulfonic samples, the signal shifted, and the intensity in the low binding energies (284 eV) slightly increased, indicating a variation in the chemical structure after decarboxylation and after a C–H bond was introduced.

A detectable signal shift for S_{2p}, F_{1s} was not found in the spectrum. For the binding energies of oxygen, two different binding states exist in perfluorosulfonic acid ionomers. Three oxygen atoms are bound in each sulfuric acid group, and two oxygen atoms on the polymer side chain are in an ether configuration for one sulfuric acid group. Thus, the O_{1s} signal was split into two peaks. The binding energies located at 533.0 and 535.7 eV were related to the oxygen in the sulfonic acid groups and in the ether configuration, respectively. The ratio for these two oxygen species decreased slightly with lower oxygen in the ether configuration after decarboxylation

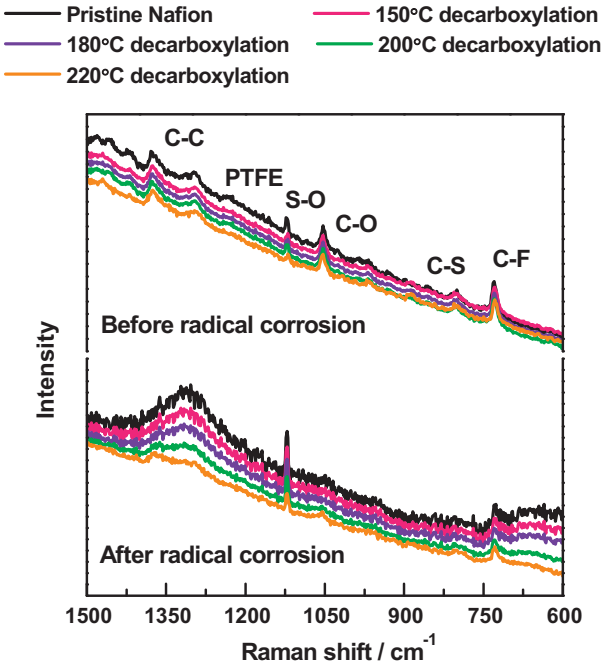

Fig. 3. Raman spectra of the perfluorosulfonic acid (top) decarboxylated at various temperatures for 24 h (bottom), after radical corrosion for 12 h.

at elevated temperatures. The lower oxygen in the ether configuration may have resulted from the activation and crystallinity of the side chain, but a definitive reason for this change remains unclear.

To investigate the possible effects of the decarboxylation treatment on the membrane performance, the EW values and proton conductivities of polymer electrolyte membranes recasted from the perfluorosulfonic acid ionomers were tested and listed in Table 1. The EW values of polymer electrolyte membranes recasted from pristine and decarboxylated ionomers were in the range of 983–1007 g mol^{-1}. The proton conductivities of the membranes recasted from the decarboxylated ionomers also displayed high values similar to the membrane recasted from the pristine ionomer, 0.096 S cm^{-1}. Taking the test deviation into consideration, the results revealed that no SO_3^- groups had decomposed from the electrolyte membrane during the decarboxylation procedure. The stability of the sulfonic groups at temperatures of 150–220 °C may be attributed to the strong electrostatic interactions of the Na^+ counter ions, which enhance the charge densities of the ion clusters and stabilize the sulfonic groups [28,29].

3.2. Chemical degradation and stability of the perfluorosulfonic acid electrolyte

Fig. 3 displays the Raman spectra of the perfluorosulfonic acid before and after radical corrosion for 12 h. The main characteristic bands located at 730, 805, 970, 1060, 1210, 1300 and 1380 cm^{-1} can be attributed to $\upsilon s(CF_2)$, υs(C–S), υs(C–O), $\upsilon s(SO_3^-)$, and υs(C–C), respectively [30]. After radical corrosion for 12 h, the vibration peaks of υs(C–S) and υs(C–O) were not observed in the Raman spectrum of the pristine perfluorosulfonic electrolyte. However, the vibration bonds of υs(C–C) increased, and the curves displayed a structure similar to that of the PTFE main chain [31]. The function groups of the decarboxylated electrolyte also revealed a decrease in intensity after radical corrosion. However, bands of υs(C–S), υs(C–O), and $\upsilon s(SO_3^-)$ were clearly observed from the spectrum of perfluorosulfonic acid that decarboxylated at 200–220 °C, demonstrating the improvement in the chemical stability after the reactions.

Table 1
EW values and proton conductivities of polymer electrolyte membranes recasting from the various perfluorosulfonic acid ionomers.

Membrane recasting from ionomer	Thickness (μm)	EW value	Proton conductivity at 25 °C, 100% RH (S cm^{-1})
Pristine ionomer	30 ± 2	1002	0.096
Decarboxylated at 150 °C	30 ± 2	993	0.095
Decarboxylated at 180 °C	30 ± 2	1007	0.097
Decarboxylated at 200 °C	30 ± 2	996	0.096
Decarboxylated at 220 °C	30 ± 2	983	0.096

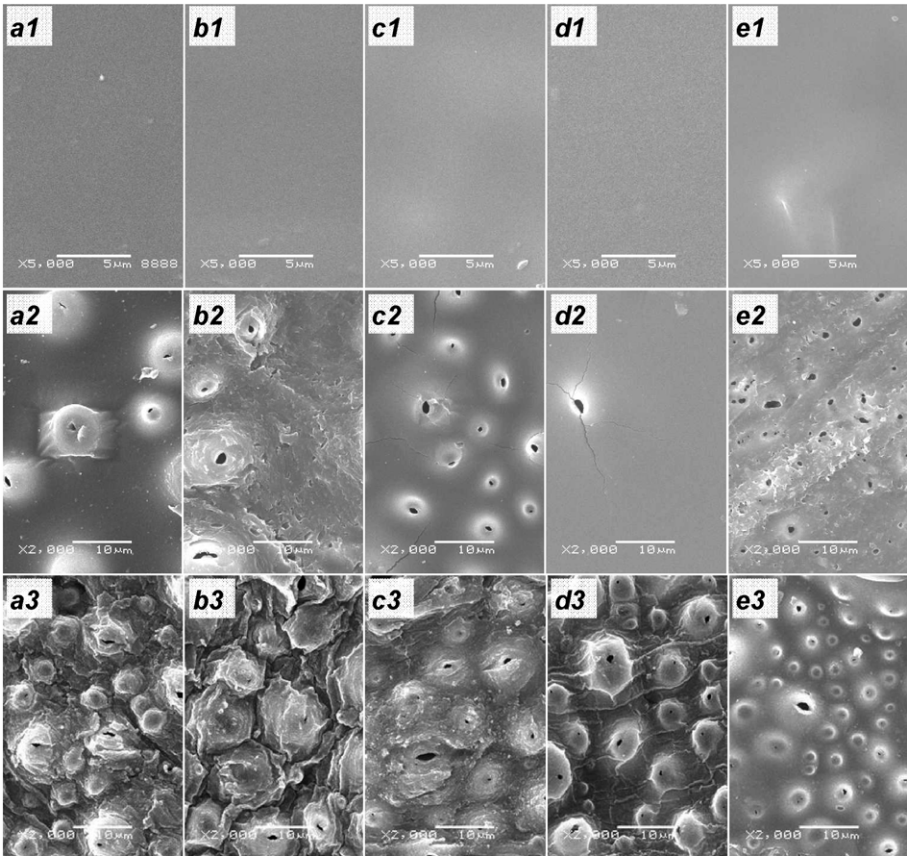

Fig. 4. SEM micrographs of the perfluorosulfonic acid (series a–e are the pristine electrolyte, the electrolyte decarboxylated at 150, 180, 200 and 220 °C for 24 h, respectively) after radical corrosion for 0 h (series 1), 6 h (series 2) and 12 h (series 3).

Fig. 4 shows the SEM micrographs of the perfluorosulfonic acid electrolytes after radical corrosion for 0 h, 6 h, and 12 h. The electrolyte membranes have smooth surface before the radical corrosion. The chemical degradation introduced several small bubbles on the electrolyte membrane surface, which gradually became pinholes during the chemical decay process. For the pristine perfluorosulfonic acid electrolytes and the electrolyte decarboxylated at 150, and 180 °C, the pinholes on the surface of the Nafion membranes were broken into pieces after 12 h, suggesting low stability and the presence of defect end groups in the polymer. As expected, the electrolyte decarboxylated at 220 °C for 24 h had the least morphological damage after corrosion.

The fluorine in the polymer was bound on the carbon in the original $(CF_2–CF_2)_n$ configuration. Therefore, the fluorine-rich carbon configurations without decomposition reflected high binding energies of approximately 292.2 eV. Degradation of the $(CF_2–CF_2)_n$ backbone of the electrolyte decreased the fluorine concentration, which caused the bonds to shift to low energy. As displayed in Fig. 5, the intensity of the peak at 292.2 eV decreased with the chemical degradation of perfluorosulfonic acid. However, the intensity of the peak at 284.2 eV increased, indicating that the relative ratio of $(CF_2–CF_2)_n$ to C–C was reduced due to the radical attack. The loss of fluorine was demonstrated by the F_{1s} high-resolution spectrum combined with decrease of the binding energies of S_{2p}. The C_{1s} spectra also displayed a dependence of the $(CF_2–CF_2)_n$ to C–C

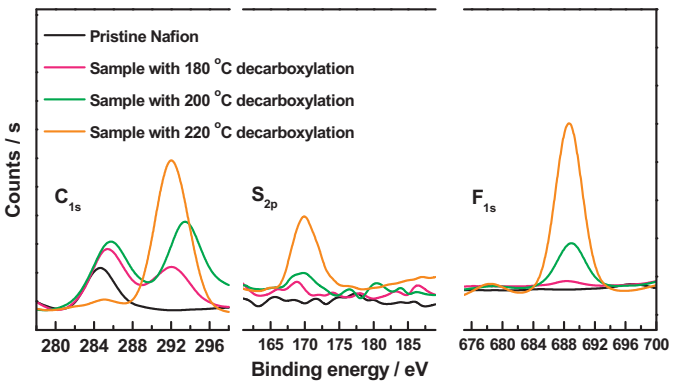

Fig. 5. C_{1s} S_{2p} and F_{1s} XPS spectra of the perfluorosulfonic acid after radical corrosion for 12 h.

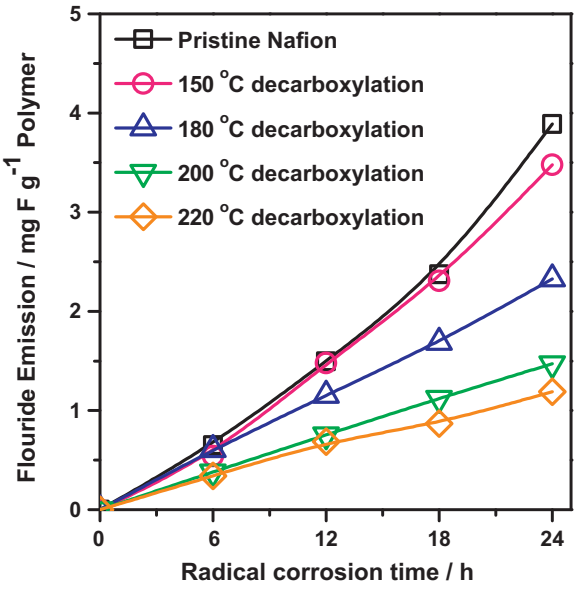

Fig. 6. Fluoride evolution from the perfluorosulfonic acid electrolytes as a function of test time under Fenton's degradation test.

relative ratio on the decarboxylated temperature of the electrolyte. The higher decarboxylated temperature resulted in a higher $(CF_2–CF_2)_n$ to C–C relative ratio and lower degradation. The spectrum of perfluorosulfonic acid decarboxylated at 220 °C for 24 h also presents a peak at 284.2 eV because of the inherent C–C and low C–H content. However, a high concentration of S_{2p} and F_{1s} remained in the perfluorosulfonic electrolyte after radical corrosion for 12 h.

3.3. Degradation kinetics of the perfluorosulfonic acid electrolytes

The fluoride generation from Nafion membrane exposed to Fenton's reagents is shown in Fig. 6. After 24 h radical corrosion, the fluoride emission was approximately 3.89, 3.48, 2.33, 1.47 and 1.20 mg for 1 g of pristine electrolyte. The perfluorosulfonic acid was decarboxylated at 150, 180, 200 and 220 °C, respectively. The results suggested that 2.4–7.8 wt.% of fluoride was released from the electrolyte membrane (F^- content in the membrane was approximately 51 wt.%). The fluoride emission rate (FER) was reduced with an increase in the decarboxylated temperature. The simulated FER for the tested samples corroded at the initial 12 h were approximately 0.109, 0.101, 0.091, 0.063, and 0.058 mg h^{-1}, respectively.

After the initial 12 h, the fluoride emission rates had an increase with increased fluoride emission/corrosion time slope for all samples. PFSA degradation processes via an unzipping mechanism through the carboxylic acid groups have been proposed in recent years. There is current debate concerning where these carboxylic acid end groups originated from. One widely accepted mechanism points to the weak polymer end groups as the initial source of carboxylic acid end groups. Another mechanism suggests that the PFSA side chain cleavage is the alternative source for the defect end groups [15,32–34]. Thus, the side chain cleavage creates additional carboxylic acid end groups on the polymer, and accelerates the degradation rate. The fluoride emission acceleration also suggests a downward trend with the improvement of decarboxylation temperature, with the total emission rate of 0.138, 0.133, 0.085, 0.049 and 0.038 mg h^{-1} for the tested samples, respectively. The low fluoride emission acceleration suggests an improved stability of the side chains at the increased temperature.

4. Conclusions

Defect carboxyl end groups of the perfluorosulfonic acid can be extensively removed by decarboxylation from the electrolyte at elevated temperature with the assistance of counter ions and ethylene glycol. Improved carboxyl conversion with increased reaction temperature demonstrates an endothermic reaction for perfluorosulfonic acid decarboxylation. Diminished carboxyl end groups are observed at 180 °C for 24 h, and lowered signals were observed at 200 and 220 °C for 24 h.

Decarboxylation of perfluorosulfonic acid significantly improves the chemical stability of the perfluorosulfonic electrolyte toward hydroperoxyl radicals. Corrosion of the pristine perfluorosulfonic electrolyte (or the electrolyte decarboxylated below 180 °C) alters the surface chemical structure similar to that of the PTFE main chain with low F^- concentration, while high concentration of the S_{2p} and F_{1s} still remained in the perfluorosulfonic electrolyte decarboxylated at 200–220 °C under the same conditions.

The decarboxylation of the electrolyte at elevated temperature improves the side chain stability of the perfluorosulfonic acid. After initial corrosion, the fluoride emission rate increases due to side chain cleavage and the additional carboxylic acid end groups on the polymer. With an increased decarboxylation temperature from 150 to 220 °C, the fluoride emission rate acceleration decreases as a function of the decarboxylation temperature.

Acknowledgements

This work was financially supported by the National High Technology Research and Development Program ("863" Program) of China (2008AA11A106 and 2009AA034400), the National Nature Science Foundation of China (50802072) and Fundamental Research Funds for the Central Universities (2010-Ia-055).

References

[1] R. Lin, B. Li, Y.P. Hou, J.M. Ma, International Journal of Hydrogen Energy 34 (2009) 2369–2376.
[2] X.J. Li, J.Q. Li, L.F. Xu, F.Y. Yang, J.F. Hua, M.G. Ouyang, International Journal of Hydrogen Energy 35 (2010) 3841–3847.
[3] A.A. Shah, T.R. Ralph, F.C. Walsh, Journal of the Electrochemical Society 156 (2009) B465–B484.
[4] N. Ohguri, A.Y. Nosaka, Y. Nosaka, Electrochemical and Solid State Letters 12 (2009) B94–B96.
[5] H.L. Tang, P.K. Shen, S.P. Jiang, W. Fang, P. Mu, Journal of Power Sources 170 (2007) 85–92.
[6] K.A. Mauritz, R.B. Moore, Chemical Reviews 104 (2004) 4535–4585.
[7] D.E. Curtin, R.D. Lousenberg, T.J. Henry, P.C. Tangeman, M.E. Tisack, Journal of Power Sources 131 (2004) 41–48.
[8] C. Zhou, M.A. Guerra, Z.M. Qiu, T.A. Zawodzinski, D.A. Schiraldi, Macromolecules 40 (2007) 8695–8707.
[9] X. Fang, P.K. Shen, S.Q. Song, V. Stergiopoulos, P. Tsiakaras, Polymer Degradation and Stability 94 (2009) 1707–1713.
[10] A.C. Fernandes, E.A. Ticianelli, Journal of Power Sources 193 (2009) 547–554.
[11] J.F. Wu, X.Z. Yuan, J.J. Martin, H.J. Wang, J.J. Zhang, J. Shen, S.H. Wu, W. Merida, Journal of Power Sources 184 (2008) 104–119.
[12] R.L. Thankamony, M.G. Lee, K. Kim, J.D. Hong, T.H. Kim, H.J. Lee, H.J. Kim, S. Nam, Y.B. Lim, Macromolecular Research 18 (2010) 992–1000.
[13] H. Ben youcef, L. Gubler, S.A. Gursel, D. Henkensmeier, A. Wokaun, G.G. Scherer, Electrochemistry Communications 11 (2009) 941–944.
[14] L. Wang, B.L. Yi, H.M. Zhang, Y.H. Liu, D.M. Xing, Z.G. Shao, Y.H. Cai, Journal of Power Sources 164 (2007) 80–85.
[15] M. Danilczuk, A.J. Perkowski, S. Schlick, Macromolecules 43 (2010) 3352–3358.
[16] M. Danilczuk, S. Schlick, F.D. Coms, Macromolecules 42 (2009) 8943–8949.
[17] F.D. Coms, H. Liu, J.E. Owejan, ECS Transactions 16 (2008) 1735–1747.
[18] G.M. Haugen, F.Q. Meng, N.V. Aieta, J.L. Horan, M.C. Kuo, M.H. Frey, S.J. Hamrock, A.M. Herring, Electrochemical and Solid State Letters 10 (2007) B51–B55.
[19] S.H. Xiao, H.M. Zhang, C. Bi, Y.N. Zhang, Y.W. Ma, X.F. Li, H.X. Zhong, Y. Zhang, Journal of Power Sources 195 (2010) 8000–8005.
[20] N.R. Gunawardena, T.B. Brill, Journal of Physical Chemistry A 105 (2001) 1876–1881.
[21] G. Marchionni, S. Petricci, G. Spataro, G. Pezzin, Journal of Fluorine Chemistry 124 (2003) 123–130.

[22] H.L. Tang, M. Pan, F. Wang, P.K. Shen, S.P. Jiang, Journal of Physical Chemistry B 111 (2007) 8684–8690.
[23] T. Xie, C.A. Hayden, Polymer 48 (2007) 5497–5506.
[24] K.M. Hutchinson, J.A. Smiley, S. Lowety-Bretz, H. Mettee, Abstracts of Papers of the American Chemical Society 227 (2004) 783–790.
[25] C. Wakai, K. Yoshida, Y. Tsujino, N. Matubayasi, M. Nakahara, Chemistry Letters 33 (2004) 572–573.
[26] S.O.C. Mundle, G. Lacrampe-Couloume, B.S. Lollar, R. Kluger, Journal of the American Chemical Society 132 (2010) 2430–2436.
[27] M. Schulze, M. Lorenz, N. Wagner, E. Gulzow, Fresenius Journal of Analytical Chemistry 365 (1999) 106–113.
[28] L.G. Lage, P.G. Delgado, Y. Kawano, Journal of Thermal Analysis and Calorimetry 75 (2004) 521–530.
[29] S.H. de Almeida, Y. Kawano, Journal of Thermal Analysis and Calorimetry 58 (1999) 569–577.
[30] Y. Tabuchi, R. Ito, S. Tsushima, S. Hirai, Journal of Power Sources 196 (2011) 652–658.
[31] A. Ohma, S. Yamamoto, K. Shinohara, Journal of Power Sources 182 (2008) 39–47.
[32] M. Danilczuk, F.D. Coms, S. Schlick, Fuel Cells 8 (2008) 436–452.
[33] N. Cipollini, ECS Transactions 11 (2007) 1071–1082.
[34] F.D. Coms, Transactions 16 (2008) 235–255.